Structure, Vibrational and Electronic Spectra, and Bonding in *trans*-Diaquabis(oxalato)vanadate(III) Complex Salts, $A[V(ox)_2(H_2O)_2]\cdot xH_2O$ (A = Cs, K, or NH_3Me), and the *X*-Ray Crystal Structure of the Potassium Salt ($x = 3$)‡

Robert Stranger,* Kamaliah Sirat, and Peter W. Smith
Chemistry Department, University of Tasmania, P.O. Box 252C, Hobart, Tasmania 7001, Australia
Ian E. Grey† and Ian C. Madsen
Commonwealth Scientific and Industrial Research Organisation Division of Mineral Products, P.O. Box 124, Port Melbourne, Victoria 3207, Australia

The *X*-ray crystal structure of potassium diaquabis(oxalato)vanadate(III), $K[V(ox)_2(H_2O)_2]\cdot 3H_2O$, has been determined [monoclinic, space group $P2/c$, with unit-cell parameters $a = 7.971(4)$, $b = 5.691(2)$, $c = 14.167(5)$ Å, $\beta = 108.97(3)°$, and $Z = 2$]. The structure has been refined to an R value of 0.032 using 560 independent reflections. In comparison with the corresponding Cs^+ and NH_3Me^+ salts, the K^+ salt exhibits a significantly longer bond distance for axially co-ordinated water and this is manifested in band shifts of 500—1 000 cm^{-1} in the visible region. For all three salts vibrational spectra and single-crystal polarised electronic spectra are reported together with assignments. Analysis of the ligand-field spectra is presented in terms of the angular overlap model. It is shown that the band shifts occurring in the electronic spectrum of the K^+ salt can be reproduced by a reduction in the σ-bonding capacity of the co-ordinated water together with a slight increase in the σ bonding of the oxalate ligand, both of which are consistent with structural differences existing between the K^+ and the other two salts. Significant anisotropy exists in the metal–oxalate π interaction with the in-plane contribution relatively small. In addition, anomalous temperature-dependent bands resulting from vibronic coupling with internal O–H stretching vibrations are present in the electronic spectra of both the Cs^+ and NH_3Me^+ salts.

Recently we reported the structure refinement of two new *trans*-diaquabis(oxalato)vanadate(III) complex salts, $A[V(ox)_2(H_2O)_2]\cdot xH_2O$, with A = Cs ($x = 4$) and A = NH_3Me ($x = 4.5$).[1] The structure of $K[V(ox)_2(H_2O)_2]\cdot 3H_2O$ has now been determined and shows distinct differences to the former two salts. However, the potassium salt is isostructural with the analogous chromium(III) salt.[2] In addition, a detailed investigation of i.r. spectra and polarised single-crystal electronic spectra has been made for these three complex salts. Both structural and spectroscopic results, together with discussion of the electronic spectra in relation to the structural and bonding differences existing between these complex salts, are now reported.

Experimental

Preparation of Compounds.—The preparation of $Cs[V(ox)_2(H_2O)_2]\cdot 4H_2O$ and $[NH_3Me][V(ox)_2(H_2O)_2]\cdot 4.5H_2O$ has been described previously.[1] The preparation of $K[V(ox)_2(H_2O)_2]\cdot 3H_2O$ follows that for the Cs salt with the exception that the cation was added in the form of potassium acetate solution and ethanol was added to initiate crystallisation. Mauve coloured crystals formed on cooling and, after filtering off and washing with acetone, were stable for prolonged periods in air (Found: C, 13.50; H, 2.90; K, 11.30; V, 14.45. Calc. for $C_4H_{10}KO_{13}V$: C, 13.50; H, 2.80; K, 10.95; V, 14.30%).

Deuteriated crystals were prepared by several recrystallisations of the appropriate complex salt from D_2O, either under vacuum or a nitrogen atmosphere.

* Author for correspondence on spectroscopic matters.
† Author for correspondence on structural matters.
‡ *Supplementary data available:* see Instructions for Authors, *J. Chem. Soc., Dalton Trans.*, 1988, Issue 1, pp. xvii—xx.

Structure Determination.—A trapezium shaped crystal was orientated along b^* using precession photographs and transferred to a Siemens AED diffractometer for the intensity data collection (Mo-K_α radiation). Lattice parameters were determined by the least-squares technique applied to the setting angles of 17 reflections with $21 < 2\theta < 45°$. A standard reflection was monitored every 50 reflections to correct for intensity drift during the data collection. Unit-cell parameters and other details of data collection are given in Table 1.

Table 1. Crystallographic data for $K[V(ox)_2(H_2O)_2]\cdot 3H_2O$

Molecular weight	356.2
Space group	$P2/c$
a/Å	7.971(4)
b/Å	5.691(2)
c/Å	14.167(5)
β/°	108.97(3)
U/Å^3	607.75
D_c/g cm^{-3}	1.95
Z	2
μ(Mo-K_α)/cm^{-1}	12.1
Crystal size (mm)	0.092 × 0.078 × 0.130
Scan type	θ—2θ
Scan width (°)	2.4 + Δθ; Δθ = $\alpha_1 - \alpha_2$ separation
Scan speed (° min^{-1})	2
Data collection range	±h, k, l, 4—40° (2θ)
No. of measured reflections	1 211
No. of independent reflections used in refinement	560
Transmission coefficients (max., min.)	0.92, 0.83
$R_{int.}$ for averaged reflections	0.013
R (unit weights; all data)	0.032

The co-ordinates of the isostructural chromium compound [2] were used as starting parameters in the refinement. Refinement of co-ordinates and anisotropic thermal parameters converged at an R value of 0.045. All hydrogen atoms were located in a difference-Fourier map. Refinement was continued with anisotropic thermal parameters for non-hydrogen atoms and an overall isotropic thermal parameter for the hydrogens. The hydrogen co-ordinates were not refined. The final R value (unit weights) for all 560 reflections was 0.032. In the final refinement, 89 parameters were varied and the largest Δ/σ was 0.03. The atomic scattering factors for neutral atoms and anomalous dispersion coefficients were taken from ref. 3. All computing was performed with the SHELX 76 system of programs [4] and ORTEP.[5] Final atomic co-ordinates are reported in Table 2; bond lengths and angles are given in Table 3.

Additional material available from the Cambridge Crystallographic Data Centre comprises H-atom co-ordinates, thermal parameters, and remaining bond lengths and angles.

Spectroscopy.—Infrared spectra were recorded at room temperature on a Digilab FTS 20E Fourier-transform spectrometer at a resolution of 4 cm^{-1}. All i.r. spectra were summed over 100 or more scans to improve the signal to noise ratio.

Polarised single-crystal electronic spectra were recorded at 18 K, and at 300 K using a Cary 17 spectrophotometer in conjunction with a Cryodyne model 21 cryostat fitted with an Oxford Instruments temperature controller and sensor.

For both Cs^+ and NH_3Me^+ complex salts, crystals formed as plates with the main crystal face being (001). Polarised spectra were obtained parallel to the crystallographic a and b axes for this face. These crystals cleaved parallel to (110) allowing polarisations parallel and perpendicular to the c axis to be obtained. The K^+ salt also grew as plates but with the (010) crystal face being best developed. This crystal face extinguished under cross-polarisers at approximately +45° from the c axis and polarised spectra were measured parallel and perpendicular to this direction. The crystal also cleaved parallel to the (100) face allowing polarisations parallel to the b and c axes to be obtained.

Table 2. Atomic co-ordinates for $K[V(ox)_2(H_2O)_2]\cdot 3H_2O$

Atom	X/a	Y/b	Z/c
K	0.0	0.651 3(3)	0.25
V	0.5	0.5	0.0
C(1)	0.311 9(7)	0.696 8(9)	0.116 3(4)
C(2)	0.777 0(7)	0.455 7(9)	0.419 6(4)
O(1)	0.555 7(4)	0.742 0(6)	0.413 2(2)
O(2)	0.713 0(4)	0.348 1(6)	0.479 3(2)
O(3)	0.256 4(5)	0.824 4(7)	0.169 4(3)
O(4)	0.896 5(4)	0.385 0(6)	0.390 1(3)
$O_w(1)$	0.656 9(4)	0.338 6(6)	0.122 8(2)
$O_w(2)$	0.873 5(4)	0.013 6(6)	0.105 6(3)
$O_w(3)$	0.5	0.170 4(8)	0.25

Table 3. Comparison of relevant bond lengths (Å) and angles (°) for $K[V(ox)_2(H_2O)_2]\cdot 3H_2O$ and $Cs[V(ox)_2(H_2O)_2]\cdot 4H_2O$*

V–O(1)	1.991(3) (*2.005*)	O(1)–V–O(2)	80.7(1) (*80.5*)
V–O(2)	2.010(4)	O(1)–V–O(2)	99.3(1)
V–O_w(1)	2.005(3) (*1.967*)	V–O(1)–C(1)	115.8(3) (*115.6*)
		V–O(2)–C(2)	115.4(3)
O(1)–O(2)	2.591(5) (*2.591*)	O(1)–C(1)–C(2)	114.0(5) (*114.1*)
O(1)–O(2)	3.048(5)	O(2)–C(2)–C(1)	113.8(5)
O(1)–O(3)	2.229(6) (*2.226*)	O(3)–C(1)–C(2)	120.5(5) (*120.0*)
O(2)–O(4)	2.233(6)	O(4)–C(2)–C(1)	120.0(5)
O(3)–O(4)	2.789(5) (*2.768*)	O(2)–C(2)–O(4)	126.2(5) (*125.9*)
		O(1)–C(1)–O(3)	125.5(5)
C(1)–C(2)	1.552(7) (*1.547*)		
C(1)–O(1)	1.281(7) (*1.290*)	O(1)–V–O_w(1)	91.0(1) (*90.1*)
C(2)–O(2)	1.277(7)	O(2)–V–O_w(1)	89.7(1)
C(1)–O(3)	1.226(8) (*1.220*)	O(1)–C–O_w(1)	89.0(1)
C(2)–O(4)	1.227(7)		
K–O(3)	2.823(5)	H-Bonded oxygens	
K–O(4)	2.824(4)		
K–O_w(1)	3.269(4)	O_w(1)–O_w(3)	2.681(4) (*2.644*)
K–O_w(2)	2.849(4)	O_w(1)–O_w(2)	2.596(5) (*2.592*)
		O_w(2)–O(4)	2.785(5)
O_w(1)–O(1)	2.800(5) (*2.591*)	O_w(2)–O(2)	2.754(5) (*2.802*)
O_w(1)–O(1)	2.851(4)	O_w(3)–O(2)	2.741(5) (*2.788*)
O_w(1)–O(2)	2.831(4)		
O_w(1)–O(2)	2.847(5)		

* Values for Cs^+ salt (ref. 1) in italics.

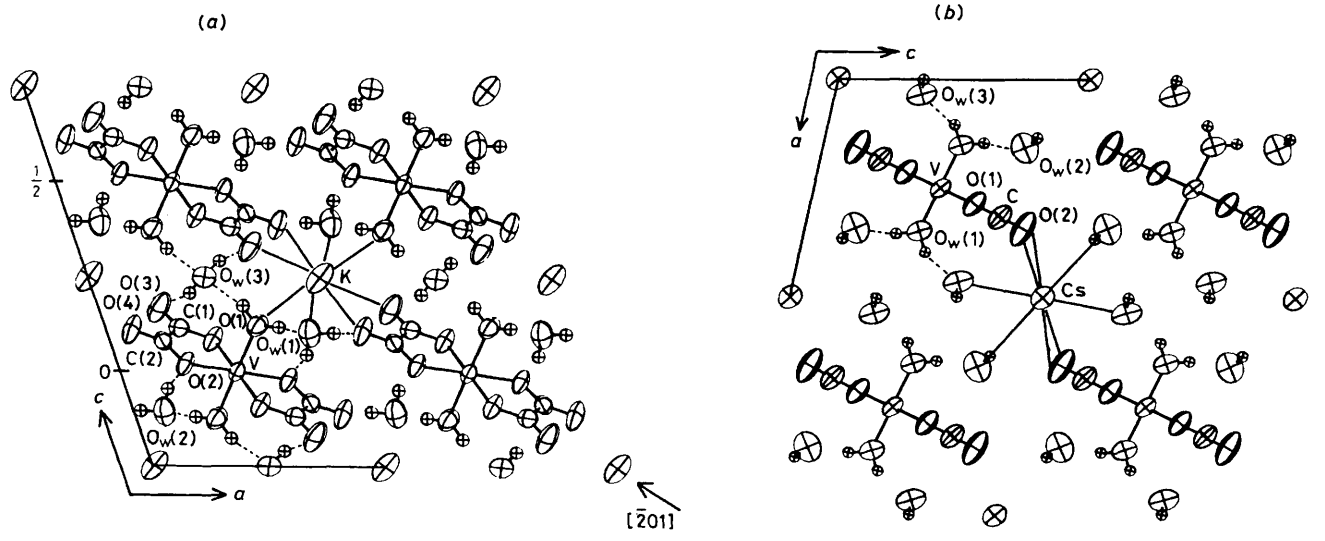

Figure 1. Structures of *trans*-diaquabis(oxalato)vanadate(III) complexes: (*a*) $K[V(ox)_2(H_2O)_2]\cdot 3H_2O$ in the (010) plane, showing chains of alternating K^+ cations and $[V(ox)_2(H_2O)_2]^-$ anions directed along [2̄01]; (*b*) $Cs[V(ox)_2(H_2O)_2]\cdot 4H_2O$ in the (010) plane

Results and Discussion

Crystal Structure.—The structure of the related potassium diaquabis(oxalato)chromate(III) complex has been described in detail by van Niekerk and Schoening.[2] Since the vanadium compound described here is isostructural, only a brief description of the structure will be given. The [010] projection of the structure, Figure 1(*a*), shows chains of alternating potassium cations and complex anions $[V(ox)_2(H_2O)_2]^-$ [ox = oxalate-(2−)], directed along [$\bar{2}$01] and held together by ionic bonds from the potassium ion to the terminal oxygens of the oxalate groups. Alternate potassium ions along [$\bar{2}$01] are displaced by 0.86 Å above and below the plane of the vanadium atoms (at $y = \frac{1}{2}$). The long symmetry axis of each of the complex anions is directed towards the potassium ions with an angle of 9° between the symmetry axis and its projection on the *ac* plane. The plane of the complex anion is tilted at 61° to the *ac* plane, with the orientation of tilt in opposite directions for alternate complex anions along [$\bar{2}$01].

Adjacent [$\bar{2}$01] chains are linked together into (010) layers by bonds involving the co-ordinated water molecules, $O_w(1)$, on complex anions in neighbouring chains, see Figure 1(*a*). These link *via* weak ionic bonds to potassium ions, K–$O_w(1)$ 3.269(4) Å, and *via* strong H-bonds to $O_w(3)$, $O_w(1)$–H · · · $O_w(3)$ 2.681(4) Å. Complex anions in successive (010) layers are linked together by strong hydrogen bonds involving the water molecules $O_w(2)$ and $O_w(3)$, as shown by the dotted lines in Figure 1(*a*).

The packing of the cations and the complex anions in the Cs^+ and NH_3Me^+ salts has a superficial resemblance to that of the K salt when the former are viewed along [010] as shown in Figure 1(*b*). However, considerable differences in detail exist. The complex anions in the Cs compound are perpendicular to the *ac* plane and the long symmetry axis of the complex ion lies in the *ac* plane at the same level as both the V and Cs ions ($y = 0$). The symmetry axis makes an angle of *ca.* 21° in the *ac* plane with the Cs–V–Cs direction, whereas in the K salt the symmetry axis is collinear with the K–V direction.

A major difference between the K and Cs salts is in the stacking of adjacent (010) layers. In the former, the layer separation corresponds to the *b* axis, 5.69 Å, and successive layers stack on top of one another. In the Cs salt, however, adjacent layers perpendicular to [010] are related by C-centring, and so the complex anions in successive layers are displaced by $\frac{1}{2}a$. The resulting co-ordination to Cs involves four bonds to terminal oxalate oxygen atoms, O(2), from complex anions in the same plane, four bonds to O(2) from complex anions in adjacent planes and two in-plane bonds to water molecules, with these ten bonds in the range 3.26—3.45 Å, as well as two longer bonds at 3.88 Å to a second water molecule. The co-ordination of Cs is thus 10 + 2 whereas that of K is 6 + 2 with pairs of bonds to O(3), O(4), and $O_w(2)$ in the range 2.82—2.85 Å and two longer bonds to $O_w(1)$ at 3.27 Å.

In Table 3 the bond lengths and angles for the K salt are given with the corresponding values for the Cs salt for comparison. All bond angles associated with the complex anions except those involving $O_w(1)$ are identical within three e.s.d.s for the two compounds. However, for the K salt, V–$O_w(1)$ [2.005(3) Å] is comparable to the average of the V–O equatorial bonds (2.000 Å), whereas for the Cs salt the axial bonds to the water molecules [1.967(3) Å] are considerably shorter than the equatorial bonds [2.005(2) Å]. This difference may be explained by the fact that the packing of the cations and complex anions, in the case of the K^+ salt, may result in weak electrostatic bonding, with K–$O_w(1)$ 3.269(4) Å, whereas in the case of the Cs^+ salt, where the shortest Cs–$O_w(1)$ distance is >5.5 Å, no such perturbation occurs. The latter circumstance also applies in the case of the NH_3Me^+ salt.

Infrared Spectra.—Proposed assignments for the observed i.r.-active fundamentals appropriate to D_{2h} molecular symmetry

Table 4. Observed i.r. frequencies* and assignments

Cs^+ salt	K^+ salt	NH_3Me^+ salt	Band assignments
3 460s,br	3 440br	3 480br	ν(O–H) B_{1u} + B_{3u}
		3 130m,br	ν(N–H)
2 960br	2 950br	2 950br	H-bonding
1 711s,sp	1 710s,sp	1 710s,sp	ν(C=O) B_{2u} + B_{3u}
1 688s,sp	1 688s,sp	1 680s,sp	
1 653s,sp	1 656s,sp	1 660s,sp	
	1 600s,br		δ(H–O–H) B_{1u}
		1 520w	δ(N–H)
		1 460m,sp	δ(C–H)
1 393s,sp	1 393s,sp	1 410s,sp	ν(C–O) + ν(C–C) B_{3u}
1 252s,sp	1 258s,sp	1 270s,sp	ν(C–O) + (O–C=O) B_{2u}
940m	975m	950m	ν(C–O) + δ(O–C=O) + ν(C–C) B_{3u}
900m	900m,sp	910m	
860m,br	855w	865m,br	$\rho_{wag}(H_2O)$ B_{2u}
800m,sp	804s,sp	810s,sp	ν(V–O) + δ(O–C=O) B_{2u}
620m	670m,sp	580(sh)	$\rho_{rock}(H_2O)$ B_{3u}
540m,sp	536s,sp	550s,sp	ν(V–O) B_{3u}
500(sh)	520(sh)	490m,sp	δ(O–C=O) + ring def. B_{2u} + ν(V–OH_2) B_{1u}(?)
410s	417s	410s	ν(V–O) + ring def. B_{2u}
380s,sp	380s,sp	375s,sp	δ(C–C=O) + ν(C–C) B_{3u}
325s	320s	330s	δ(O–V–O) out-of-plane B_{1u}
255sp	251s	255s	ring def. B_{3u} + δ(H_2O–V–OH_2) B_{2u} or B_{3u}(?)
—	240s	—	
227s	210s	228s	δ(H_2O–V–OH_2) B_{2u} or B_{3u}

* s = Strong, m = medium, w = weak, br = broad, sp = sharp, sh = shoulder; def. = deformation.

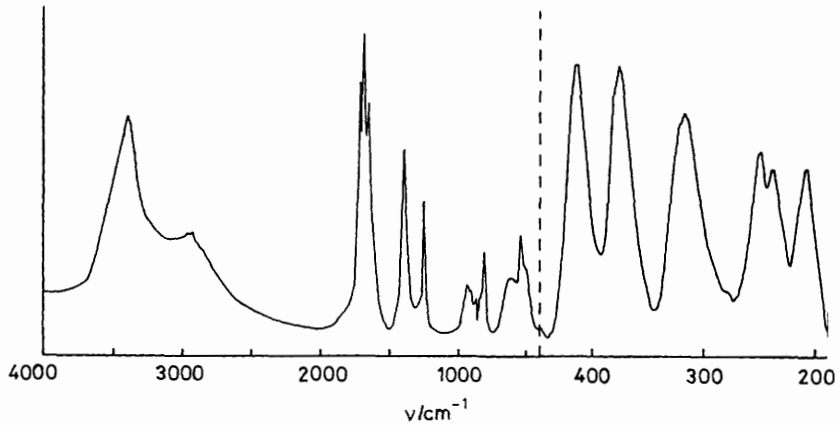

Figure 2. Infrared spectra of *trans*-diaquabis(oxalato)vanadate(III) complexes: for the Cs^+ salt, 4 000—450 cm^{-1}; for the K^+ salt, 450—200 cm^{-1}

are given in Table 4 for the spectral range 4 000—200 cm^{-1}; the spectra for the Cs^+ and K^+ salts are shown in Figure 2.

The internal modes of the $[V(ox)_2(H_2O)_2]^-$ ion for D_{2h} molecular symmetry span the representations shown below.

$$\Gamma_v = 9A_g + 6B_{1g} + 5B_{2g} + 4B_{3g} + 4A_u + 6B_{1u} + 8B_{2u} + 9B_{3u}$$

Neglecting the co-ordinated water, the vibrations associated with the $V(ox)_2$ entity can be grouped into 23 in-plane modes (contained within the metal–oxalate plane) spanning $6A_g + 5B_{1g} + 6B_{2u} + 6B_{3u}$, and 10 out-of-plane modes spanning $2B_{2g} + 2B_{3g} + 3A_u + 3B_{1u}$. The 18 remaining vibrations are attributed to internal modes involving the co-ordinated water as well as vibrations which result in deformation of both V–O(ox) and V–OH_2 bonds. Of a total of 51 internal modes, 23 are i.r. active, these latter being of B_{1u}, B_{2u}, and B_{3u} symmetry type only.

The vibrational assignments reported in Table 4 are largely based on earlier work by Nakamoto and co-workers[6] for related bis-oxalato complexes where a normal co-ordinate analysis was carried out for the in-plane vibrations of the $[Pt(ox)_2]^{2-}$ ion. In addition, Gouteron[7] has given detailed assignments for the in-plane vibrations observed for the *trans*-$[Ir(ox)_2Cl_2]^{3-}$ anion. For vibrations involving the co-ordinated water, the assignments of McCarthy and co-workers[8,9] for the $[V(H_2O)_4Cl_2]^+$ species serve as a useful guide. Although not included in Table 4, the i.r. spectra of $K_3[V(ox)_3]\cdot 3H_2O$ and the deuteriated salt of $[NH_3Me][V(ox)_2(H_2O)_2]\cdot 4.5H_2O$ were also measured down to 450 cm^{-1} further to aid vibrational assignments, in particular, to discriminate between co-ordinated water- and oxalate-based vibrations.

For all three salts studied here the site symmetry of the complex anion is lower than D_{2h} but in each case the centre of symmetry is still retained; the appropriate site symmetries are C_{2h}, C_i, and C_{2h} for the Cs^+, K^+, and NH_3Me^+ salts, respectively. Correlation from D_{2h} molecular symmetry reveals that no additional fundamentals or site group splitting of molecular modes are expected, with the exception of the previously inactive A_u modes, which become i.r. active in C_i site symmetry applicable to the potassium salt. However, correlation field effects will result in unit-cell splitting of molecular modes which may be observable in the i.r. spectra of these salts.

Assignment of observed fundamentals down to 350 cm^{-1} is relatively straightforward for in-plane V^{3+}–oxalate vibrations since band positions are close to those reported for related complexes.[6,7,10] Correlation field splitting is particularly prominent for B_{2u} and B_{3u} molecular modes involving the ν(C=O) internal co-ordinate. Specifically, for the Cs^+ salt seen in Figure 2, three components are well resolved between 1 650 and 1 710 cm^{-1}. Correlation from D_{2h} to C_{2h} site symmetry through to C_{2h}^3 ($Z = 2$) unit-cell symmetry results in a doubling of all i.r.-active modes. As such, four i.r. unit-cell modes are possible for this co-ordinate of which three are actually observed. Correlation field splitting is also observed for the B_{3u} mode involving a mixture of ν(C–O), ν(O–C=O), and ν(C–C) co-ordinates between 890 and 975 cm^{-1}.

The moderately intense band observed in the far-i.r. between 320 and 330 cm^{-1} is assigned to an out-of-plane oxalate vibration of B_{1u} symmetry rather than a V–OH_2 based vibration on account of a similar band being observed for both $[Cu(ox)_2]^{2-}$ and $[Pt(ox)_2]^{2-}$ at around 330 cm^{-1}.[10] From the normal co-ordinate analysis of the $[Pt(ox)_2]^{2-}$ ion, a mode involving in-plane deformation of the oxalate ring was calculated to lie at 200 cm^{-1}. However, Gouteron[7] observed this band in *trans*-$[Ir(ox)_2Cl_2]^{3-}$ at 264 cm^{-1}, therefore the band observed around 250 cm^{-1} for the complex salts studied here may be tentatively assigned to this vibration and as B_{3u}.

The assignments for vibrations involving the co-ordinated water are fairly unambiguous at least down to 350 cm^{-1}. The δ(H–O–H) deformation mode of B_{1u} symmetry is obscured by the more intense ν(C=O) vibrations around 1 650 cm^{-1} for the Cs^+ and NH_3Me^+ salts. However, the band is resolved as a lower energy shoulder in the K^+ salt and is observed to move to 1 170 cm^{-1} in the deuteriated NH_3Me^+ salt. The bands located at around 860 and 600 cm^{-1} also shift to 670 and 430 cm^{-1} in the deuteriated salt. These may be tentatively assigned to the wagging B_{2u} and rocking B_{3u} modes, respectively, if the inverse assignments of Adams and Lock[11] are used. The band or shoulder observed between 490 and 520 cm^{-1} may also be assigned to the B_{1u} asymmetric V–OH_2 stretch since the analogous E_u vibration in the $[V(H_2O)_4Cl_2]^+$ ion was observed at 521 cm^{-1}.[9] The in-plane and out-of-plane (VO_4) vibrations associated with the alkali salts of $[V(H_2O)_4X_2]^+$ (X = Cl or Br) were observed between 208 and 290 cm^{-1}. As such, bands observed between 200 and 250 cm^{-1} for the oxalate complexes studied here may also be tentatively assigned to δ(H_2O–V–OH_2) modes of B_{2u} and B_{3u} symmetry. It is also possible that the two unassigned out-of-plane B_{1u} vibrations associated with the co-ordinated oxalate are also contributing to this spectral region. Finally, the remaining B_{3u} vibration involving the δ(ox–V–ox) co-ordinate is assumed to lie below 200 cm^{-1} since from the normal co-ordinate analysis of $[Pt(ox)_2]^{2-}$ the vibration is calculated to lie at 65 cm^{-1}.

Electronic Spectra.—Polarised electronic spectra were measured at 18 and 300 K on single crystals of $Cs[V(ox)_2(H_2O)_2]\cdot 4H_2O$, $[NH_3Me][V(ox)_2(H_2O)_2]\cdot 4.5H_2O$, and

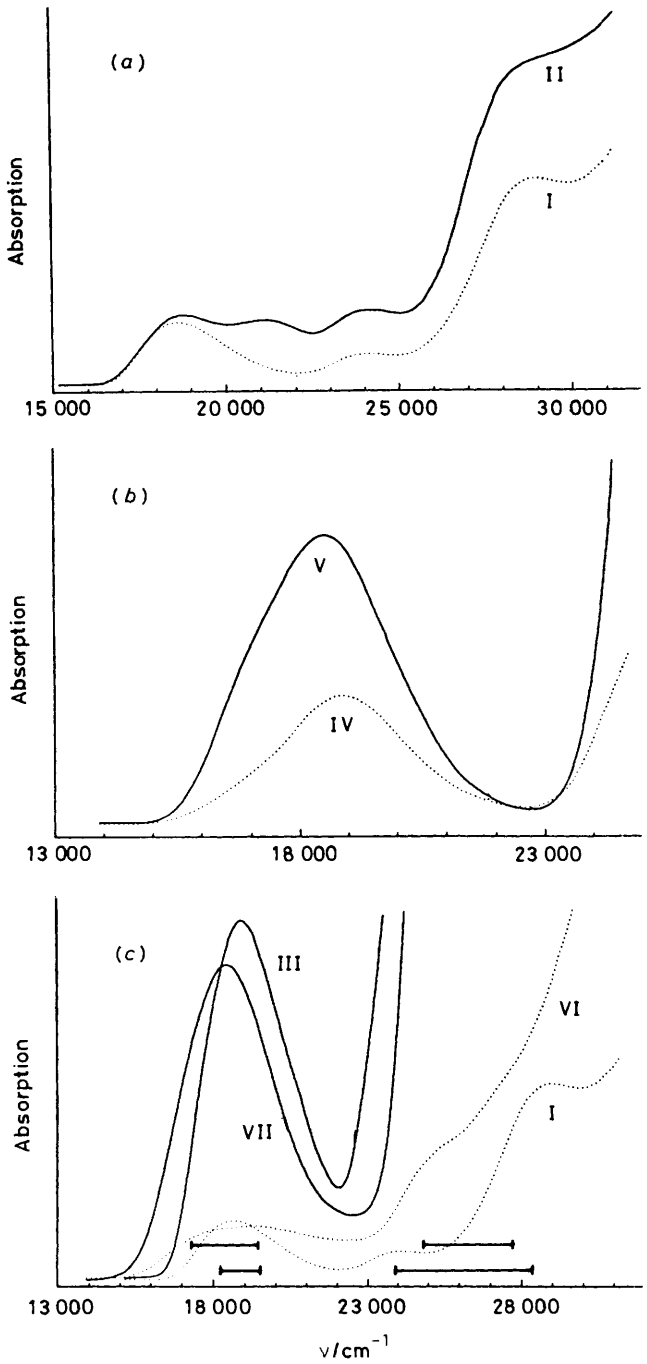

Figure 3. Polarised single-crystal electronic spectra of *trans*-diaquabis(oxalato)vanadate(III) complexes: (*a*) measured on the (001) crystal face of the NH_3Me^+ salt [polarisations I ($E_{\parallel}a$) and II ($E_{\parallel}b$)]; (*b*) measured on the (100) crystal face of the deuteriated K^+ salt [polarisations IV ($E_{\parallel}b$) and V ($E_{\parallel}c$)]; (*c*) comparison of polarised spectra for K^+ [polarisations VI (E 45° from c) and VII (E −45° from c)] and NH_3Me^+ [polarisations I ($E_{\parallel}a$) and III ($E_{\parallel}c$)] salts

$K[V(ox)_2(H_2O)_2]\cdot 3H_2O$ as well as on the deuteriated analogues of the latter two salts. (Since the polarised spectra of the Cs and NH_3Me^+ salts were almost identical, only the results for the NH_3Me^+ and K^+ salts are given here for illustration.) Figure 3(*a*) shows the spectra obtained for the (001) crystal face of the NH_3Me^+ salt with the electric vector parallel to the crystallographic *a* and *b* axes (spectra I and II, respectively).

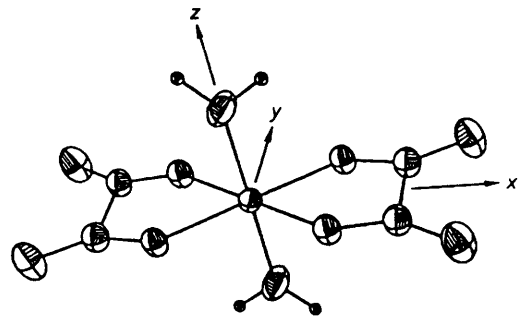

Figure 4. Structure and molecular co-ordinate system for the $[V(ox)_2(H_2O)_2]^-$ chromophore

Table 5. Contribution of molecular spectra to crystal polarisation directions

Polarisation		Molecular spectra *x*	*y*	*z*
NH_3Me^+ salt	I	0	1	0
	II	0.056	0	0.944
	III	0.944	0	0.056
K^+ salt	IV	0.030	0.751	0.220
	V	0.531	0.043	0.425
	VI	0.002	0.219	0.778
	VII	0.968	0.030	0.002

Figure 3(*b*) shows the spectra measured on the (100) crystal face for the deuteriated K^+ salt with the electric vector parallel to the crystallographic *b* and *c* axes (spectra IV and V, respectively). In Figure 3(*c*) similar polarisation directions with respect to the $[V(ox)_2(H_2O)_2]^-$ chromophore are compared for the NH_3Me^+ (spectra I and III) and K^+ salts (spectra VI and VII). Polarisations VI and VII were measured on a (010) face of the K^+ salt while polarisation III was obtained from the (110) face of the NH_3Me^+ salt with the electric vector parallel to the crystallographic *c* axis. The relative contributions of molecular *x*, *y*, and *z* spectra to these polarisation directions are given in Table 5 with respect to the co-ordinate system given in Figure 4. They were calculated as averages over the different orientations of the $[V(ox)_2(H_2O)_2]^-$ chromophores in each unit cell.

An examination of Figure 3 in conjunction with Table 5 reveals that the molecular *x* spectrum, where the electric light vector bisects the metal–oxalate bite angle, is clearly dominant in intensity for both salts. Also, disregarding the 21 300 cm^{-1} band in polarisation II of Figure 3(*a*), it is apparent that the molecular *y* and *z* spectra are quite similar with respect to both band maxima and overall intensity. Perhaps the most obvious difference in the spectra is the shift of *ca.* 600 cm^{-1} to lower energy of the first band in the K^+ salt in relation to the analogous band in the NH_3Me^+ salt. This shift is particularly evident for the most intense polarisation seen in Figure 3(*c*). Furthermore, the low symmetry splitting of this band has undergone a significant increase in the K^+ salt whereas the splitting between the two highest energy bands shows a marked decrease with respect to the corresponding bands in the NH_3Me^+ salt.

For the NH_3Me^+ salt, the $[V(ox)_2(H_2O)_2]^-$ anion possesses almost exact D_{2h} molecular symmetry. However, the K^+ salt deviates from D_{2h} symmetry in the following respects. First, the two V–O bond lengths associated with a single oxalate ligand are no longer equal. Secondly, the two oxalate ligands no

longer lie in the same plane and therefore neither is orthogonal to the V–OH_2 axis. Finally, the H–O–H plane associated with the co-ordinated water no longer lies within the molecular *xz* plane but has been rotated around *z* so that it lies in an intermediate position. However, for both salts the $[V(ox)_2(H_2O)_2]^-$ chromophore still remains centrosymmetric, therefore all *d–d* transition intensity must be vibronically induced through coupling with *ungerade* vibrations. To a good approximation only metal–ligand vibrations need be considered, the remaining vibrations which are largely localised on either the oxalate or water ligands can be ignored. Hence, in deriving vibronic selection rules only the vibrations associated with the VO_6^{3-} entity need be specified. For this unit the internal vibrations for D_{2h} symmetry span the representations shown below. Since these vibrations span all D_{2h} representations, then

$$\Gamma_v(VO_6) = 3A_{1g} + B_{1g} + B_{2g} + B_{3g} + A_{1u} + 2B_{1u} + 3B_{2u} + 3B_{3u}$$

all *d–d* transitions are vibronically allowed in all three polarisations. In this respect, it is not possible to make any definitive statement about band assignments on the merits of polarisation data alone. It is therefore necessary to use intuitive chemical arguments to estimate the relative magnitudes of ligand-field parameters in order to determine the likely splitting of cubic ligand field states. In the ligand-field analysis to follow, the band positioned at *ca.* 21 300 cm^{-1} in polarisation II of Figure 3(*a*) was excluded for reasons which will be discussed later.

Estimation of A.O.M. (Angular Overlap Model) Ligand-field Parameters.—On the basis of spectrochemical arguments it is anticipated that the ligand-field strength of the co-ordinated water will be slightly higher than that for the oxalate group. It is possible however, to obtain an estimate of the ratio $e_\sigma^{O_w}/e_\sigma^{ox}$ from the known values of $10Dq$ for the hexa-aqua[12] and tris-oxalato[13] complexes of V^{3+}, these being 18 400 and 17 500 cm^{-1}, respectively. Assuming that e_π/e_σ is the same for both water and oxalate ligands, one obtains the value $e_\sigma^{O_w}/e_\sigma^{ox} = 1.05$. The value of e_π/e_σ for co-ordinated water shows considerable variation from one complex to another.[14] Perhaps the most reliable estimate should come from the value of e_π/e_σ for co-ordinated water in Cr^{3+} systems since not only is the oxidation state of the metal ion the same but also $10Dq$ for the hexa-aqua ions of V^{3+} and Cr^{3+} are very similar. For Cr^{3+}, e_π/e_σ is quite low having a value of 0.18.[15]

From the above parameter ratios and known $10Dq$ value for hexa-aqua V^{3+}, it is a simple matter to obtain the following estimates for the angular overlap parameters in $[V(ox)_2(H_2O)_2]^-$: $e_\sigma^{O_w} \sim 7\,000$ cm^{-1}, $e_\sigma^{ox} \sim 6\,700$ cm^{-1}, $e_\pi^{O_w} \sim 1\,300$ cm^{-1}, and $e_\pi^{ox} \sim 1\,200$ cm^{-1}, with the Racah *B* value of *ca.* 640 cm^{-1} being that found for the hexa-aqua V^{3+} ion. It should be noted that in the above parameter estimates, negligible in-plane π bonding for both water and oxalate ligands has been assumed. If this is not the case, then the e_σ parameters will accordingly increase in value.

Ligand-field Calculations and Band Assignments.—The calculations in relation to the observed spectra were carried out in the framework of the angular overlap model (a.o.m.) using the FORTRAN program CAMMAG.[16] To aid these calculations, polarisations I and VI shown in Figure 3(*c*) were subjected to Gaussian analysis in order to resolve low-symmetry components, particularly for the lowest energy band centred around 18 500 cm^{-1}. Calculations were complicated by the fact that π

Table 6. Observed and calculated ligand-field transition energies (cm^{-1}) and assignments

	Calculated *		Assignment (D_{2h})			
Observed	(*a*)	(*b*)	(*a*)	(*b*)	Cubic parent	Ligand-field parameters (cm^{-1})
NH_3Me^+ salt:	0	0	B_{2g}	B_{2g}		I
	2 441	252	B_{3g}	B_{3g}	$^3T_{1g}$	$e_\sigma^{O_w} = 7\,275$
	3 785	3 259	B_{1g}	B_{1g}		$e_\sigma^{ox} = 6\,525$
						$e_{\pi\perp}^{O_w} = 1\,125$
18 213	17 956	18 210	A_{1g}	A_{1g}		$e_{\pi\perp}^{ox} = 1\,000$
	18 508		B_{3g}		$^3T_{2g}$	$B = 630$
19 519	19 492	19 390	B_{2g}	B_{2g}		II
		19 880		B_{3g}		$e_\sigma^{O_w} = 7\,975$
						$e_\sigma^{ox} = 7\,125$
23 937	23 978	23 958	B_{1g}	B_{1g}		$e_\pi^{O_w} = 900$
28 366	28 298	28 442	B_{2g}	B_{3g}	$^3T_{1g}(P)$	$e_{\pi\perp}^{ox} = 975$
	28 447	29 815	B_{3g}	B_{2g}		$B = 630$
	36 773	38 742	B_{1g}	B_{1g}	$^3A_{2g}$	
K^+ salt:	0	0	B_{2g}	B_{2g}		I
	2 229	308	B_{3g}	B_{3g}	$^3T_{1g}$	$e_\sigma^{O_w} = 6\,800$
	3 451	3 104	B_{1g}	B_{1g}		$e_\sigma^{ox} = 6\,625$
						$e_{\pi\perp}^{O_w} = 975$
17 320	17 243	17 405	A_{1g}	A_{1g}		$e_{\pi\perp}^{ox} = 950$
	18 528	19 286	B_{3g}	B_{2g}	$^3T_{2g}$	$B = 645$
19 365	19 362	19 716	B_{2g}	B_{3g}		II
						$e_\sigma^{O_w} = 7\,450$
ca. 24 800	24 533	24 393	B_{1g}	B_{1g}		$e_\sigma^{ox} = 7\,150$
ca. 27 700	27 579	27 837	B_{3g}	B_{3g}	$^3T_{1g}(P)$	$e_\pi^{O_w} = 800$
	28 047	29 217	B_{2g}	B_{2g}		$e_{\pi\perp}^{ox} = 975$
						$B = 645$
	36 355	38 010	B_{1g}	B_{1g}	$^3A_{2g}$	

(*a*) Anisotropic case with $e_{\pi\parallel}^{O_w} = 0$ and $e_{\pi\perp}^{O_w}$ non-zero. (*b*) Isotropic case with $e_{\pi\parallel}^{O_w} = e_{\pi\perp}^{O_w}$. * For all calculations $e_{\pi\parallel}^{ox} = 0$ and $\zeta_{3d} = 0$.

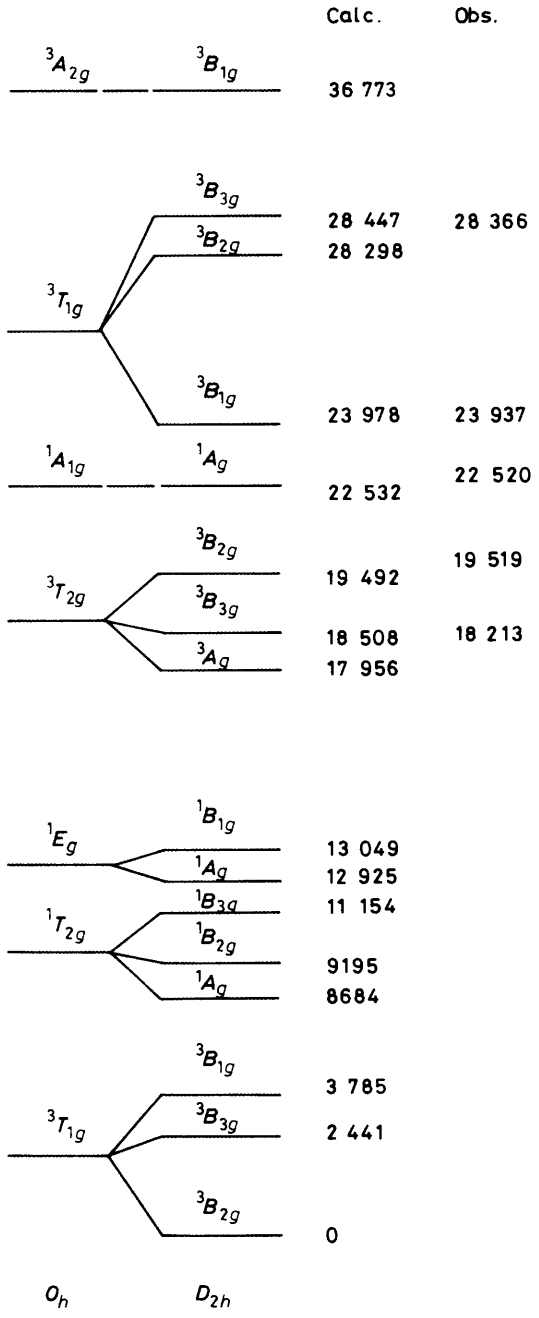

Figure 5. A.o.m. state energies calculated for the NH_3Me^+ salt with parameter values $e_\sigma^{O_w} = 7\,275$, $e_\sigma^{ox} = 6\,525$, $e_{\pi\perp}^{O_w} = 1\,125$, $e_{\pi\perp}^{ox} = 1\,000$, $B = 630$, $C = 2\,450$ cm^{-1}, and $\zeta_{3d} = 0$. Assignments given are for D_{2h} molecular symmetry

bonding anisotropy, resulting from the non-linear ligation of both water and oxalate ligands, increases the number of a.o.m. ligand-field parameters to six, excluding the Racah B parameter. Clearly, since only four spectral bands are observed a unique fit is not possible unless certain restrictions are made. In this respect, calculations were performed where the in-plane π bonding parameter ($e_{\pi\parallel}$) for both water and oxalate ligands was set either equal to the out-of-plane contribution (isotropic case) or set to zero (anisotropic case). In the final calculations two sets of optimisations were undertaken for both the NH_3Me^+ and K^+ salts where the in-plane π bonding associated with the co-ordinated water was set either to zero (a) or equal to the out-of-plane contribution (b). The final results are reported in Table 6 where the best-fit Gaussian components to the observed bands are compared with the calculated energies.

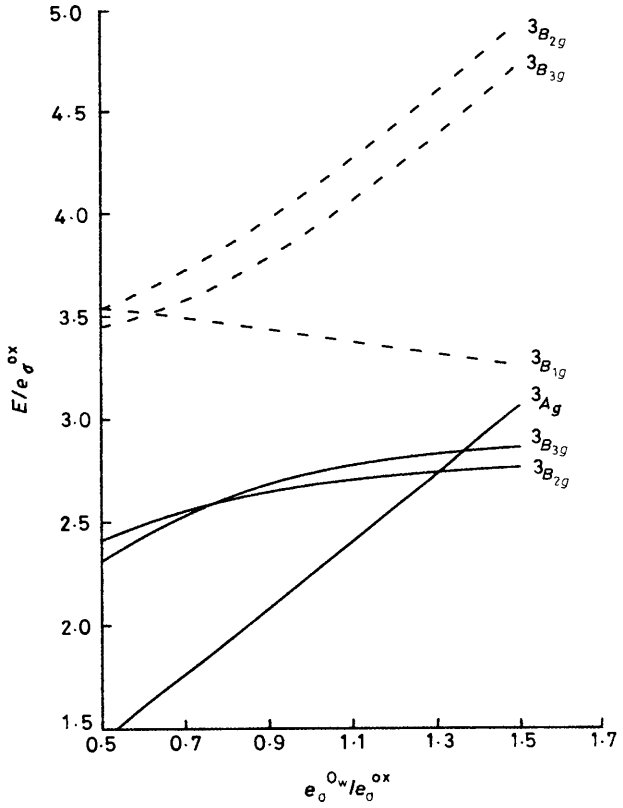

Figure 6. Energy dependence (E/e_σ^{ox}) of D_{2h} components of $^3T_{2g}$ (——) and $^3T_{1g}(P)$ (– – –) cubic states as a function of $e_\sigma^{O_w}/e_\sigma^{ox}$

An additional calculation was carried out using the complete d^2 basis in order to refine the Racah C parameter to fit the observed spin singlet state at *ca.* 22 520 cm^{-1} in the NH_3Me^+ salt. The a.o.m. parameters and the Racah B value used in this calculation were those refined in the anisotropic case for the NH_3Me^+ salt above. The results of this calculation are given in Figure 5 where the energy levels resulting from the ligand-field splitting of the free ion terms are matched with their calculated energies. For simplicity, spin-forbidden transitions involving electron occupation of formally cubic e_g orbitals are omitted in Figure 5.

Initially, an attempt was made to assign the three observed spectral bands at *ca.* 18 500, 24 000, and 28 500 cm^{-1} in polarisation I of Figure 3(*a*), to transitions from the $^3T_{1g}$ ground state to $^3T_{2g}$, $^3T_{1g}(P)$, and $^3A_{2g}$ cubic states respectively. However, in the cubic approximation these bands cannot be fitted for acceptable values of $10Dq$ and the Racah B parameter. It is therefore necessary to assign two of these bands to low-symmetry components of either $^3T_{2g}$ or $^3T_{1g}(P)$, the $^3A_{2g}$ state lying to much higher energy and therefore obscured by charge-transfer bands.

The splitting of $^3T_{2g}$ and $^3T_{1g}(P)$ cubic states for the Cs^+ salt as a function of $e_\sigma^{O_w}/e_\sigma^{ox}$ is given in Figure 6. In these calculations the in-plane π-bonding parameter ($e_{\pi\parallel}^{ox}$) for the oxalate ligand was set to zero whereas isotropic π bonding was assumed to hold for the metal–water interaction. From Figure 6 it is apparent that even for $e_\sigma^{ox} = e_\sigma^{O_w}$ significant splitting of $^3T_{2g}$ and $^3T_{1g}(P)$ cubic states occurs. This splitting results largely from the anisotropic metal–oxalate π interaction but also, to a lesser extent, from the deviation of the chelate bite

angle from 90°. Similar calculations, but with the π bonding isotropic for the oxalate ligand ($e_{\pi\parallel}^{ox} = e_{\pi\perp}^{ox}$), resulted in much smaller splittings of the above cubic states, particularly for $^3T_{2g}$, and this is in conflict with the observed spectra.

Assuming that $e_\sigma^{O_w} \geqslant e_\sigma^{ox}$, one may predict from Figure 6 that the low symmetry splitting of $^3T_{1g}(P)$ will be greater than that for $^3T_{2g}$. As such, the bands positioned at 23 940 and 28 370 cm^{-1} in Figure 3(*c*) are both assigned to components of $^3T_{1g}(P)$, while the lowest energy band centred at *ca.* 18 500 cm^{-1} is assigned to components of $^3T_{2g}$. In this respect, the large observed splitting of $^3T_{1g}(P)$ is indicative of significant anisotropy in the metal–oxalate π interaction with the in-plane contribution relatively small. Relatively small in-plane π-bonding contributions from other non-linear ligating ligands have also been reported.[14,15]

The estimation of the π-bonding anisotropy for the co-ordinated water is more difficult. Results from other studies show that in general $e_{\pi\parallel}$ is less than $e_{\pi\perp}$ by *ca.* 50%, although cases have arisen where $e_{\pi\parallel} \simeq e_{\pi\perp}$.[14] However, recently the $^3T_{1g}$ ground states of both the caesium and ammonium V^{3+} alums were shown to have large axial splittings of *ca.* 2 000 cm^{-1}.[17] Similar splittings of *ca.* 1 500 cm^{-1} in the excited states have been observed in the optical spectrum of $(NH_4)V(SO_4)_2 \cdot 12H_2O$ and were shown to result from a negligible in-plane π-bonding contribution of the co-ordinated water.[18]

On the whole, good agreement occurs between observed and calculated transition energies for the NH_3Me^+ salt for both isotropic and anisotropic π bonding of the co-ordinated water. In addition, the best fit angular overlap parameters obtained, as well as the Racah *B* value, are in good agreement with the initial estimates derived above from the hexa-aqua and tris-oxalato complexes of the V^{3+} ion. It is not possible to make any reliable statement regarding the π-bonding anisotropy of the co-ordinated water except that overall, considering both NH_3Me^+ and K^+ salts, slightly better agreement occurs for the anisotropic case. For both isotropic and anisotropic π bonding of the co-ordinated water, the parameter ratio $e_\sigma^{O_w}/e_\sigma^{ox}$ remained stable at a ratio of 1.12 for the NH_3Me^+ salt and 1.03 for the K^+ salt. These ratios are in agreement with spectrochemical arguments based solely on $10Dq$ and confirm that the ligand-field strength of co-ordinated water is slightly greater than that for the oxalate ligand. The ratio e_π/e_σ, although low, is similar for both water and oxalate ligands and gave an average value of *ca.* 0.14 over both NH_3Me^+ and K^+ salts. As anticipated, the values of $e_\sigma^{O_w}$ and e_σ^{ox} increase significantly in the isotropic case.

Band Shifts and Bonding Differences in $[V(ox)_2(H_2O)_2]^-$ *Salts.*—The band shifts apparent in Figure 3(*c*) must be accounted for on the basis of structural differences between the $[V(ox)_2(H_2O)_2]^-$ chromophores existing in the two salts. The major difference between the two structures is a lengthening of the V–O_w(1) bond by 0.050 Å in the K^+ salt as well as a slight decrease in the average V–O(ox) bond length by 0.017 Å. Consideration of these structural changes would suggest that the major alteration in ligand-field parameters would be a reduction in $e_\sigma^{O_w}$ and a small increase in e_σ^{ox}. The Racah *B* value may also undergo a slight increase as the overall metal–ligand overlap has decreased.

Examination of Figure 6 shows that the $^3T_{2g}(A_g)$ component will undergo a significant shift to lower energy if $e_\sigma^{O_w}$ is reduced thus increasing the splitting within the $^3T_{2g}$ cubic state. Conversely, the splitting within the $^3T_{1g}(P)$ cubic state is expected to decrease since both $^3B_{2g}$ and $^3B_{3g}$ components will move sharply to lower energy. Looking at Figure 3(*c*) all the above predicted band shifts are observed in going from the NH_3Me^+ to the K^+ salt. However, the significant shift of the $^3T_{1g}(B_{1g})$ component from 23 940 cm^{-1} to approximately 24 700 cm^{-1} in the K^+ salt cannot be accounted for simply on the basis of a reduction in the $e_\sigma^{O_w}$ parameter. This higher energy shift largely results from an increase in either the Racah *B* value or e_σ^{ox} parameter. To obtain the observed band shifts an unrealistic increase in *B* is required and this seems chemically unreasonable. On the other hand, a relatively small increase in the e_σ^{ox} parameter will result in a significant shift to higher energy of the $^3B_{1g}$ component and this is consistent with the observed V–O(ox) bond length decrease in the K^+ salt. As such, for the anisotropic case, a reduction in $e_\sigma^{O_w}$ by 475 cm^{-1} and an increase in e_σ^{ox} by 100 cm^{-1}, as well as minor changes in the e_π and Racah *B* parameters, reproduces the observed band shifts giving good agreement between observed and calculated energies. Furthermore, the relative changes in the e_σ parameters between the two salts are compatible with the known bond length differences.

Anomalous Electronic Bands.—The band positioned at *ca.* 21 300 cm^{-1} in both the NH_3Me^+ and Cs^+ salts, polarisation II in Figure 3(*a*), exhibits unusual properties. First, unlike all other observed spectral bands, this transition is completely polarised along the molecular *z* axis corresponding to the V–O bond associated with the co-ordinated water. Secondly, the band displays anomalous temperature dependence uncharacteristic of normal vibronically induced electric dipole transitions. In this respect, whereas all other observed bands increase in intensity on warming, this particular band loses intensity, being most intense at lowest temperatures. Finally, on deuteriation of the NH_3Me^+ salt, this band moves *ca.* 1 000 cm^{-1} to lower energy.

Similar behaviour of such anomalous bands has been observed in other complex hydrates,[19–21] in particular, for the recently studied $Cs_3VCl_6 \cdot 4H_2O$ complex salt containing the *trans*-$[VCl_2 \cdot 4H_2O]^+$ chromophore.[8] For this complex the anomalous band was attributed to a phonon sideband involving the symmetric O–H stretching vibration associated with the co-ordinated water. It is also possible however, that the band intensity is derived, at least in part, from a *ungerade* metal–ligand mode coupled to an O–H stretching vibration which removes the centre of symmetry existing in the chromophore. For the $[V(ox)_2(H_2O)_2]^-$ anion, the O–H stretching vibrations span A_g, B_{2g}, B_{1u}, and B_{3u} representations. Consideration of vibronic selection rules operating on the ground and excited electronic states obtained from the a.o.m. calculations indicates that both mechanisms are able to contribute intensity to the molecular *z* polarisation, the B_{3u} O–H stretching mode being active if the latter mechanism applies. However, the fact that this band is absent in other polarisations, as well as its anomalous temperature dependence, suggests that whatever mechanism is operative, it is lattice dependent and as such sensitive to hydrogen bonding existing between the co-ordinated water and water of crystallisation in the unit cell (see Figure 1).

The same phenomenon is most likely present in the K^+ salt, but due to overlap with neighbouring transitions the anomalous band is not obviously resolved. However, evidence for its existence in the K^+ salt can be inferred from a comparison of the weaker polarisation in the spectra of the deuteriated and non-deuteriated salts. Comparing polarisations IV and VI in Figure 3(*b*) and (*c*) respectively, it is clear that the higher energy band component positioned at *ca.* 19 000 cm^{-1} has undergone a significant intensity enhancement in relation to the lower energy component at *ca.* 17 300 cm^{-1} in the deuteriated salt, whereas both components are of comparable intensity in the non-deuteriated salt. Both polarisations are mixtures of molecular *y* and *z* spectra with the molecular *x* spectrum virtually absent. For the NH_3Me^+ salt it is known that molecular *y* and *z* polarisations are very similar; therefore it can be concluded that the observed intensity enhancement is largely the result of a

lower energy shift of the anomalous band on deuteriation such that it now lies close to the band component around 19 000 cm^{-1}.

Acknowledgements

We thank the C.S.I.R.O.–University of Tasmania Collaborative Research Fund for financial support, also, within the University of Tasmania, the Central Science Laboratory for the use of Fourier-transform i.r. and cryostat facilities and Dr. Michael Hitchman and Robbie McDonald, Chemistry Department, for access to other spectroscopic facilities and for helpful discussions. Two of us gratefully acknowledge the receipt of postgraduate awards from the Commonwealth of Australia (to R. S.) and the Malaysian Government (to K. S.).

References

1 I. E. Grey, I. C. Madsen, K. Sirat, and P. W. Smith, *Acta Crystallogr., Sect. C*, 1985, **41**, 681.
2 J. N. van Niekerk and F. R. L. Schoening, *Acta Crystallogr.*, 1951, **4**, 35.
3 'International Tables for *X*-Ray Crystallography,' Kynoch Press, Birmingham, 1974, vol. 4.
4 G. M. Sheldrick, SHELX 76, Program for Crystal Structure Determination, University of Cambridge, 1976.
5 C. K. Johnson, ORTEP, Report ORNL-3794, Oak Ridge National Laboratory, Tennessee, U.S.A., 1965.
6 J. Fujita, A. E. Martell, and K. Nakamoto, *J. Chem. Phys.*, 1961, **36**, 331.
7 J. Gouteron, *J. Inorg. Nucl. Chem.*, 1976, **38**, 55.
8 P. J. McCarthy, J. C. Lauffenburger, P. M. Skonezny, and D. C. Rohrer, *Inorg. Chem.*, 1981, **20**, 1571.
9 D. Michalska-Fong, P. J. McCarthy, and K. Nakamoto, *Spectrochim. Acta, Sect. A*, 1983, **39**, 835.
10 J. Fujita, A. E. Martell, and K. Nakomoto, *J. Chem. Phys.*, 1961, **36**, 324.
11 D. M. Adams and P. J. Lock, *J. Chem. Soc. A*, 1971, 2801.
12 K. Nakamoto and P. J. McCarthy, 'Spectroscopy and Structure of Metal Chelate Compounds,' John Wiley, New York, 1968.
13 T. S. Piper and R. L. Carlin, *J. Chem. Phys.*, 1961, **35**, 1809.
14 A. Bencini, C. Benelli, and D. Gatteschi, *Coord. Chem. Rev.*, 1984, **60**, 131.
15 D. W. Smith, *Struct. Bonding (Berlin)*, 1978, **35**, 87.
16 D. A. Cruse, J. E. Davies, M. Gerloch, J. H. Harding, D. J. Mackey, and R. F. McMeeking, 'CAMMAG, a FORTRAN Computer Package,' University Chemical Laboratories, Cambridge, 1979.
17 S. P. Best and R. J. H. Clark, *Chem. Phys. Lett.*, 1985, **122**, 401.
18 M. A. Hitchman, R. G. McDonald, R. Stranger, and P. W. Smith, *J. Chem. Soc., Dalton Trans.*, in the press.
19 J. Ferguson and T. E. Wood, *Inorg. Chem.*, 1975, **14**, 184, 190.
20 P. J. McCarthy, J. C. Lauffenburger, P. M. Skonezny, and D. C. Rohrer, *Inorg. Chem.*, 1981, **20**, 1566.
21 G. E. Shankel and J. B. Bates, *J. Chem. Phys.*, 1976, **64**, 2539.

Received 12*th January* 1987; *Paper* 7/052